RIVER ICE COVER INFLUENCE ON SEDIMENT TRANSPORTATION AT PRESENT AND UNDER PROJECTED HYDRO-CLIMATIC CONDITIONS

Kämäri Maria[1,3], Alho Petteri[2,4], Veijalainen Noora[3], Aaltonen Juha[3], Huokuna Mikko[3], Lotsari Eliisa[1]

[1]University of East Finland, Yliopistokatu 2 P.O. Box 111, FI-80101, Joensuu Finland
[2]Department of Geography & Geology, University of Turku, 20014 Turun yliopisto, Finland
[3]Finnish Environment Institute, SYKE, Mechelininkatu 34a, P.O. Box 140, FI-00251, Helsinki, Finland e-mail: maria.kamari@ymparisto.fi, Telephone: +358 2952 51334
[4]Department of Real Estate, Planning and Geoinformatics, AALTO University, P.O.Box 15800, 00076 AALTO

ABSTRACT

A large number of rivers are frozen annually and the river ice cover has an influence on the geomorphological processes. These processes in cohesive sediment rivers are not fully understood. Therefore, this paper demonstrates the impact of river ice cover on sediment transport, i.e. turbidity, suspended sediment loads and erosion potential, compared with a river with ice-free flow conditions. The present sediment transportation conditions during the annual cycle are analysed, and the implications of climate change on wintertime geomorphological processes are estimated. A one-dimensional hydrodynamic model has been applied to the Kokemäenjoki River in SW Finland. The shear stress forces directed to the river bed are simulated with present and projected hydro-climatic conditions. The results of shear stress simulations indicate that a thermally formed smooth ice cover diminishes river bed erosion, compared with an ice-free river with similar discharges. Based on long-term field data, the river ice cover reduces turbidity statistically significantly. Furthermore, suspended sediment concentrations measured in ice-free and ice-covered river water reveal a diminishing effect of ice cover on riverine sediment load. The hydrodynamic simulations suggest that the influence of rippled ice cover on shear stress is varying. Climate change is projected to increase the winter discharges by 27–77 % on average by 2070–2099. Thus, the increasing winter discharges and possible diminishing ice cover periods both increase the erosion potential of the river bed. Hence, the wintertime sediment load of the river is expected to become larger in the future.

1. INTRODUCTION

In many regions, the river-ice exists for a significant part of the year and induces geomorphological changes (Zabilansky *et al.*, 2006; Turcotte *et al.*, 2011). An unresolved issue is whether river ice has an evident effect on channel morphology (Ettema and Kempema, 2013), and the influence of ice cover on river bed morphology is not fully examined. Considering the importance and the role of river ice as a geomorphological agent on morphodynamic processes, the spatial and temporal aspects must be considered (Boucher *et al.*, 2012).

Sediment transport processes depend on how the ice cover modifies the flow distribution, which in turn depends on the type and variability of the cover (Beltaos and Prowse, 2009). Turcotte et al. (2011) reviewed studies indicating that the sediment transport capacity of a river channel reduces due to a stable

ice cover, but the influence of ice cover on the amount of sediment supplied to the channel has not been thoroughly explored. Already, in the 1970s it was found that under ice cover, the sediment transport rate was reduced, mainly due to the lower velocities (Sayre and Song, 1979). On the other hand, a fixed ice cover may intensify bed erosion (Zabilansky *et al.*, 2006), especially if a bank-fast and rough ice cover is restrained from responding vertically to changes in discharge. The average water velocity is reduced by the additional ice-water boundary. Given that the total shear boundary must be divided between the water-bed and water-ice interfaces, a reduced drag on the channel bed can be expected. Additional influence of ice cover on sediment processes are connected to lateral redistribution of flow and reduced velocity of secondary currents (Ettema and Daly, 2004).

The changes in suspended sediment concentrations are not totally controlled by the components in the river channel itself, but also by the surrounding catchment area (Schumm, 1973; Puustinen *et al.*, 2007; Malve *et al.*, 2012). Pouring rain and runoff may temporally magnify the suspended sediment loads transported in the river as particles are washed from the drainage basin.

The river bed sediment properties have an important role in the analysis of the erosion potential of a river. The Kokemäenjoki River bed sediments are dominated by cohesive soils and fine sand (Cripps *et al.*, 2011; Lotsari *et al.*, 2014). The force needed to initiate movement of sediment particles, i.e. critical shear stress, is dependent on the size, shape and density of a particle, and its position in the river bed (Chow, 1959). In cohesive sediments, the resistance to erosion depends also on the strength of the cohesive bond between the particles (Chow, 1959; Hassanzadeh, 2012).

Historically, river ice cover periods have shortened, and the interannual variability in both freeze and breakup dates has increased in the northern hemisphere (Magnuson *et al.*, 2000). In the future, a continued reduction in ice duration is expected in all Northern regions (Prowse *et al.*, 2011). Global sea level rise is expected in connection with climate change. The projected sea level rise of the Baltic Sea (Johansson *et al.*, 2014), where the gently sloping Kokemäenjoki River enters, is partly compensated for to the land uplift that is still ongoing after the last ice age in SW Finland. These changes will modify the forces applied to the river bed in the future.

The **aim of the study** is to examine ice cover impact on turbidity and erosion potential at present and in the projected future conditions. We define the erosion potential as changes in shear stress applied on the river bed by flowing water. We analyse 1) turbidity and 2) sediment load variation as well as 3) average winter shear stress based on long-term monitoring data of the last 40 years. 4) Variation of the wintertime shear stresses in 2070–2099 is also calculated. The erosion potential of the river bed is simulated with the aim of a hydrological and a hydrodynamic model. Projected changes in shear stress will be based on extreme and average climate projections. The future trend in seasonal riverine sediment load variation is projected based on long-term suspended solids monitoring data and climate scenarios. The main focus is on average winter period processes along with related aspects of the seasonal and annual cycles.

2. STUDY AREA

The lower reach of the Kokemäenjoki River in Southwest Finland was selected as a case study area (Figure 1). The regulated and 121 km-long river drains a 27 000 km^2 area before it flows into the Bothnian Sea, which is the largest sub-basin of the Baltic Sea. Presently, the water quality of the coastal areas in the eastern part of the Bothnian Sea has been degraded (HELCOM, 2010). The Kokemäenjoki River is a major source of sediment and nutrients (Räike *et al.*, 2003) for the sea in SW Finland. In addition, heavy metals and polychlorinated biphenyls in the river bed sediments (Cripps *et al.*, 2011) pose a risk for the marine environment.

The thermal winter lasts on average for 100 days in SW Finland (Vehviläinen and Huttunen, 1997; Drebs *et al.*, 2002), but variability between years is high. Hydrology is characterized by snow accumulation in winter and snow melt in spring. On average, spring is the time of the largest discharges, but floods can occur during all seasons. Winter floods are not uncommon during mild winters.

The water level of the Kokemäenjoki River is extensively monitored on a national level and operationally forecasted, because the city of Pori (Figure 1) is vulnerable to flooding from the river (Huokuna, 2007;

Koskinen, 2008). In addition to river discharge, sea level and wind conditions also have influence on the river water level in Pori. The river is regulated by four dams, and the main storage capacity is within the lakes in the upstream catchment area. The lowest reach of the river is controlled by the Harjavalta dam (Figure 1) and a hydro-electric power plant. The monthly mean discharge in Harjavalta during the period 1931–2012 has been within the range 30–680 m^3s^{-1} and the highest discharge was 918 m^3s^{-1} on 5th of May 1966. The Loimijoki tributary enters the Kokemäenjoki River upstream of Harjavalta (Figure 1). It is a major source of suspended sediments to the Kokemäenjoki River, especially during peak discharges when waters of the main river are stored in upstream lakes. The catchment area of Loimijoki comprises 35 % fields, which is greater when compared with the 16 % of the whole Kokemäenjoki River catchment (Räike *et al.*, 2003).

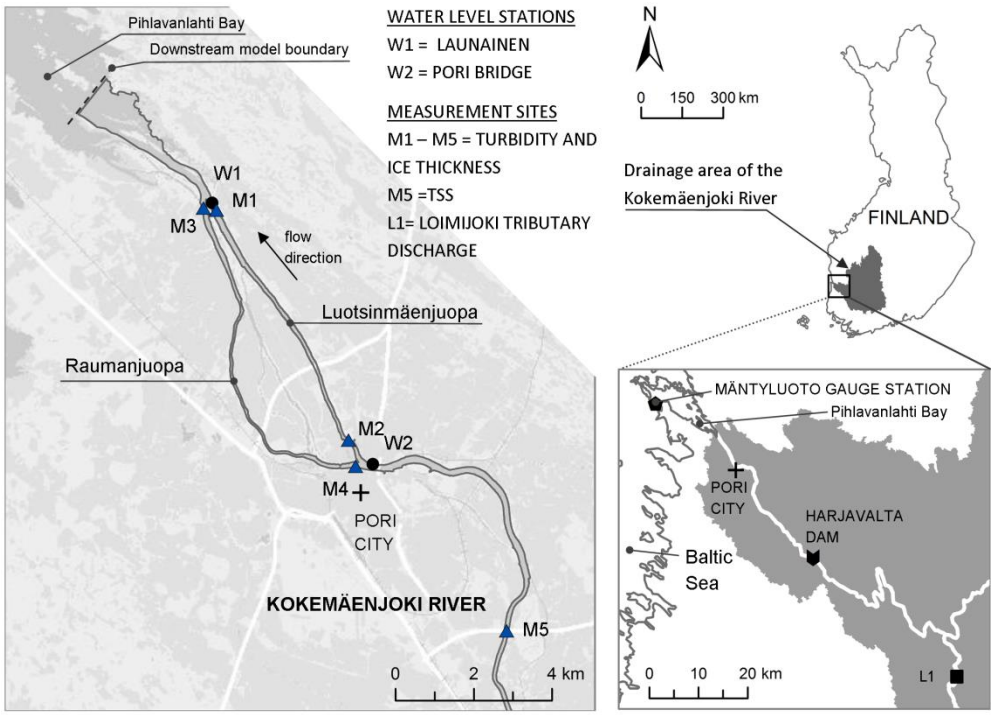

Figure 1. Lower reach of the Kokemäenjoki River, turbidity, suspended solid water sampling locations and ice thickness monitoring sites M1–M5. Automated river water level stations W1 and W2 exist in Launainen and Pori Bridge. The coastal sea level is monitored with an automated Mäntyluoto gauge station operated by the Finnish Meteorological Institute. Discharge is measured in Harjavalta and in the Loimijoki tributary

Representative riverbed sediment types in the studied river reach are fine sand, cohesive silt and clay size particles (Cripps *et al.*, 2011; Lotsari *et al.*, 2014). There is more erosion than deposition in the lowermost 39 km of the main channel and distributaries (Lotsari *et al.*, 2014). The suspended river sediments are largely deposited in Pihlavanlahti Bay (Niinikoski, 2011). Since the 17th century, the rate of river mouth movement forward towards the sea has been varying between 14 and 80 m/year (Cripps *et al.*, 2011).

3. MATERIAL AND METHODS

A range of field data and methods were applied for the purpose of analysing ice cover influence on sediment processes in the present winter conditions, and to estimate the future changes (Figure 2). These are presented in more detail in the following sections.

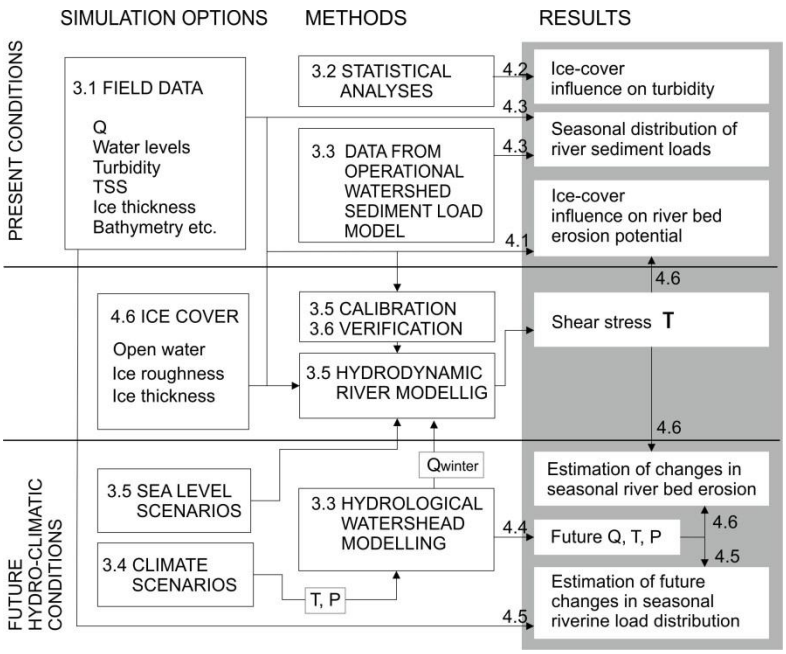

Figure 2. Schematic presentation of the main components of the study. Numbers refer to the titles of this article

3.1 Field data

The water quality of the Kokemäenjoki River is monitored at several sites. The Finnish Environmental Administration collect samples 4 to 12 times per year. Simultaneously, the river ice thickness has been measured when present. The turbidity, suspended solid, river discharge, water level and ice observation data (Figure 1) were extracted from a national environment information system (HERTTA) by the Finnish Environmental Administration, accessible to the public via the internet.

The turbidity was determined from each water sample by the nefelometric method in an accredited laboratory. The unit for turbidity is a Formazing Nephelometric Unit (FNU). The turbidity observations of the ice-covered river were compared with the turbidity of ice-free river water with similar discharges during 1973–2013. The spring period was left out of the comparison, while suspended sediment load to the river from the watershed was the largest during the spring freshet.

Total suspended solids (TSS) data (N=313) from monitoring station M5, as well as monthly mean discharges from Harjavalta, from 1990–2013, were used to estimate riverine sediment load. A 40 μm pore size polycarbonate filter was applied in the gravimetric analysis to measure solids suspended in water samples in an accredited laboratory.

The Kokemäenjoki River and Loimijoki tributary daily discharges were extracted for the periods 1971–2014 and 1971–2013 respectively. The influence of the Loimijoki tributary on the turbidity levels of the main river was analysed based on discharge variations. For hydrodynamic model verification purposes, hourly discharge from the Harjavalta power plant was provided by Pohjolan Voima Ltd for the period from mid-November to the end of December, 2007. Water level observations from automated stations W1 and W2 (Figure 1) were also utilized in the verification runs.

Ice cover thickness data (N=391) are available from sites M1–M5 for the period 1968–2013. The data give an overall view of the ice conditions in the lower reach of the Kokemäenjoki River. The maximum observed ice thickness has been 90 cm (Figure 3). The lower reach of the Kokemäenjoki River may be ice-free during the months January–February, indicating a late freeze-up date, mid-winter thaws or an early ice break-up date. The number of no-ice observations was 23 during those two months.

Ice break-up took place in the city of Pori between 6 February and 21 April for the monitoring period 1983–2013. The mean break-up date was 2 April. A coherent time series of river ice formation does not exist for the river but, during winter 2013–14, the ice cover formation and melt were monitored with a web camera placed on the river bank in Pori city. Pictures were taken every 2nd hour, and the information of the ice cover formation was used as background data in the hydrodynamic model verification.

The bathymetric data for hydrodynamic modelling were obtained from two sources. An echo-sounder measurement campaign in the Kokemäenjoki River was conducted by the Finnish Environment Institute in 2003, and the data were applied to a downstream stretch 0–4 km from the estuary. For the stretch 4–39 km from the estuary, we applied multibeam echosounder data surveyed by Kemijoki Aquatic Technology Oy in 2010 (Lotsari *et al.*, 2014). The river bed elevation data were combined with river bank elevation, to create a Triangulated Irregular Network (TIN). The discharge divergence between the distributaries Luotsinmäenjuopa and Raumanjuopa was determined based on Acoustic Doppler Current Profiler flow measurements (Lotsari *et al.*, 2014). The information was used in steady state hydrodynamic simulations.

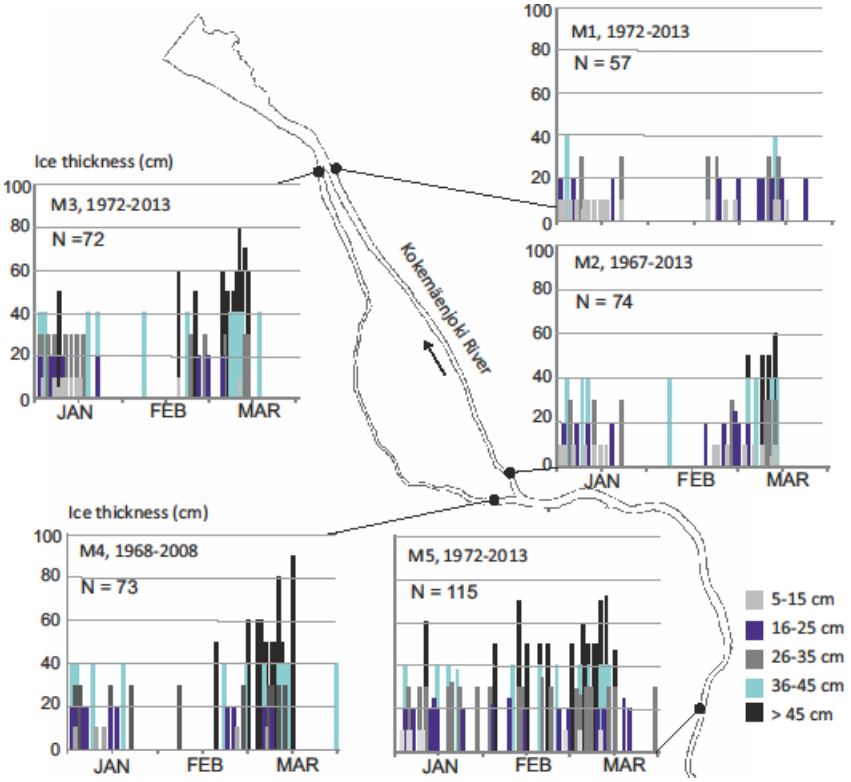

Figure 3. Ice thickness observations in the lower reach of the Kokemäenjoki River. N denotes the number of observations

3.2 Statistical analyses

We compared the observed turbidity of ice-free periods to the turbidity of the ice-covered river water. The research hypothesis is that a river ice cover is reducing water turbidity. The available turbidity data was divided into groups according to daily mean river discharge, season and the ice circumstances of the river. We have calculated the mean and standard deviation of the turbidity for different groups. The difference of mean turbidity was tested with an independent samples Student's t-test when the number of turbidity data was sufficiently large. Equal variances were not assumed in the t-test.

3.3 Hydrological river discharge and sediment load modelling

The future daily discharges of the Kokemäenjoki River were simulated using the hydrological model Watershed Simulation and Forecasting System (WSFS), which is an HBV-type (Bergström, 1976) conceptual rainfall-runoff model consisting of small lumped sub-catchments (Vehviläinen, 2007). The WSFS has been used in several studies to evaluate the effects of climate change on water resources (Vehviläinen and Huttunen, 1997; Lotsari *et al.*, 2010; Veijalainen *et al.*, 2010a; Veijalainen *et al.*, 2010b). An operational version of WSFS is used for flood forecasting and regulation planning in Finland. The Nash-

Sutcliffe efficiency criterion (NSE) (Nash and Sutcliffe, 1970) for the control period 1971–2000 was 0.74 for daily discharge at Harjavalta.

The national scale operational nutrient and suspended sediment load model VEMALA (Huttunen *et al.*, submitted) was used to estimate the riverine suspended sediment loads for the period 1990–2013. VEMALA is based on the WSFS hydrological model and was developed further for simulation of nutrient and sediment load processes. It calculates daily averages of riverine suspended sediment loads. The erosion and/or sedimentation of solids are calculated in three sub-models. The terrestrial sub-model calculates the sediment load from agricultural and non-agricultural areas. The lake sub-model calculates the mass balance of nutrients and sediments and the river sub-model simulates the river bed erosion and sedimentation. The operational model is automatically calibrated for all water quality measurement points. Details and verification results of the VEMALA modelling system can be found from Huttunen et al. (submitted).

The future sediment load for the different climate change scenarios was calculated using a regression function, which related the Kokemäenjoki River daily sediment load estimates, derived from observed TSS concentrations, and daily discharges for 1990–2013. The best estimate for the sediment load (L_s, t/day) was obtained by fitting the sediment load separately for ice-free (1) and ice-covered (2) river discharges:

$$L_s = 0.0442Q^{1.6122}, \qquad r^2=0.71 \qquad (1)$$

$$L_s = 0.0021Q^{1.9659}, \qquad r^2=0.82 \qquad (2)$$

where Q is the daily mean discharge (m^3s^{-1}). The variation of sediment loading is explained better for the lower discharges than for those above 350 m^3s^{-1}, while the load variation in higher discharge situations becomes larger and the amount of available TSS data smaller (Figure 4). An additional source of uncertainty in the use of equations (1) and (2) is that they do not take into account possible future changes in the land use practices or other factors that might result in a different erosion regime.

3.4 Climate scenarios

Five climate scenarios based on A1B greenhouse gas emission scenario are used in this study. These scenarios were selected from an ensemble of 20 climate scenarios and cover the range of uncertainty associated with climate change. The scenarios ARPEGE-HIRHAM, HadCM3-HadRm, ECHAM-RCA3 and HAdCM3-RCA3 include a regional climate model. The GLOB scenario is an average of 19 global climate models with A1B emission scenario (Ruosteenoja and Jylhä 2007). Temperature and precipitation for the periods 2010–2039, 2040–2069, 2070–2099 and 1971-2000 as reference period are used as an input for the WSFS. The delta change approach was used to transfer the climate signal of the climate models to the WSFS (Hay *et al.*, 2002; Veijalainen *et al.*, 2010b).

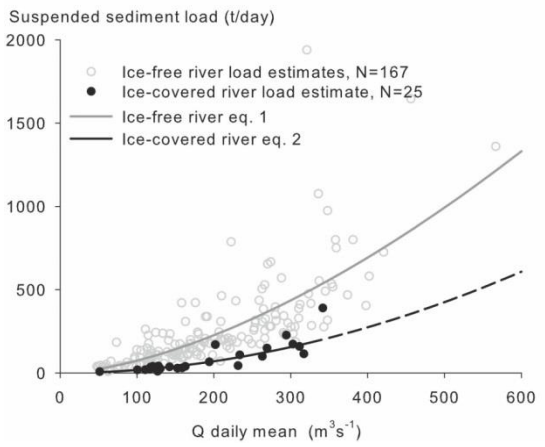

Figure 4. Scatter plot of daily riverine sediment load versus river discharge and fitted regression lines

3.5 Hydrodynamic modelling of shear stress changes

Hydrodynamic steady state simulations are performed with a 1-D HEC-RAS model (Brunner, 2010) to calculate shear stress variations in the Kokemäenjoki River in different ice, flow and sea level conditions. When water flows in a river, a force is developed that acts in the direction of flow on the channel bed. A tangential force per unit area is defined as the shearing stress. The shear stress (τ) was obtained from the following equation (Brunner, 2010):

$$\tau = \gamma R S_e, \quad (3)$$

where, R is the hydraulic radius of the channel, S_e the slope of energy grade line and γ is the unit weight of water. R was calculated with equations 4 and 5 in open water and ice conditions respectively:

$$R = \frac{A}{P} \quad (4)$$

$$R_i = \frac{A_i}{P_b + B_i} \quad (5)$$

where A is the cross-sectional area, P the wetted perimeter of a channel cross section, A_i the flow area beneath the ice cover, P_b the wetted perimeter associated with the channel bottom and banks under ice cover, and B_i the width of the underside of the ice cover. The composite roughness of an ice-covered channel n_c is calculated in HEC-RAS with the Belokon-Sadaneev formula:

$$n_c = \left(\frac{n_b^{3/2} + n_i^{3/2}}{2}\right)^{2/3} \quad (6)$$

where n_b is the river bed Manning's roughness value (n-value), and n_i the ice n-value.

We compare the influence of smooth thermally formed ice cover as well as rippled ice cover of different thicknesses on τ compared to open channel flow. The plausible n-values of these two types of ice covers are 0.012 (smooth) and 0.03 (rippled/rough) (Brunner, 2010). Thereby, the possible range of hydraulic resistance of the river ice cover is captured in the simulations. n_i can range from 0.01 for smooth ice cover in mid-winter, to 0.03 for pre-breakup conditions when heat transfer has developed three-dimensional roughness features in the ice (Carey, 1966; Carey, 1967; Beltaos, 1995).

When the critical shear stress (τ_{crit}) of particles on the bed is exceeded, particles move. τ_{crit} values on level bottoms are in the range 1.4–6.1 Nm^{-2} and on average 2.8 Nm^{-2} in the Kokemäenjoki River calculated by Lotsari et al. (2014), based on methods presented by Chow (1959) and Lick et al. (2004). Critical tractive force of cohesive soils can range from 1 Nm^{-2} for loose soils up to 30 Nm^{-2} for very compact sandy clays (Chow, 1959).

The model set-up constitutes a 39 km-long river reach that, in the city of Pori, divides into two distributaries. TIN was exported to the HEC-RAS to create 445 cross sections altogether for the model. The bathymetric model set-up is the same as used by Lotsari et al. (2014), but it has been extended ~ 4 km further downstream with the 2003 echo-sounder data. We used the same calibrated n_b-values within the range 0.02–0.04 as Aaltonen (2006) and Lotsari et al. (2014).

A uniform ice cover extending from the river estuary to the Harjavalta dam is applied in steady state ice cover simulations. Present status simulations are forced by the present mean winter discharge and sea level conditions. The range of winter average shear stress for the period 2070–2099 is simulated with varying upstream discharge boundary conditions derived from the WSFS simulated discharges. The average, high and low sea level scenarios for 2100 at Mäntyluoto (Johansson *et al.*, 2014), are taken into account in the calculation of the downstream water level boundary values. The water level in the monitoring station W1, which is the closest to the model boundary, is influenced both by the sea level fluctuation and by the Kokemäenjoki River discharge. Lotsari et al. (2014) introduced the best fit equation (7) to produce water levels of Launainen (WL_{W1}, m) from Mäntyluoto sea levels (SL, m) and Harjavalta discharge (Q, m^3s^{-1}):

$WL_{W1} = SL + 0.00076Q - 0.02663, \quad r^2 = 0.63 \quad (7)$

The downstream boundaries for the climate scenario simulations are derived from the equation (7).

3.6 Hydrodynamic model verification

The hydrodynamic model set-up was verified against observed water levels for the period from mid-November to the end of December 2007. The upstream boundary condition was the hourly discharge from Harjavalta. Hourly water level observations from W1 (Figure1) were used as the lower boundary condition. The mean absolute and maximum deviations between the simulated and observed hourly water levels in Pori were 4 cm and 17 cm respectively. NSE was calculated to be 0.95 and indicated a very good performance level of the model to produce the water levels in Pori during open water conditions (Moriasi *et al.*, 2007). In the unsteady verification run, the HEC-RAS model divided the discharge in between the distributaries. On average, 33 % of the flow was conveyed by the Raumanjuopa distributary and 67 % by the Luotsinmäenjuopa distributary. The simulated discharge divergence values corresponded to the discharge divergence measurement by Lotsari et al. (2014), and were used in steady flow shear stress simulations.

A thermally formed ice cover existed in the river 19–30 January 2014, according to the web-camera information. The model set-up was verified against observed water levels during that ice-covered period. Skim ice started to form on 13 January 2014, and the next day a solid ice cover existed in the river in Pori. The air temperature was below −4°C for the rest of the month (Figure 5) and the ice cover was gradually thickening until the end of the verification period. In addition to weather conditions, the hydropower companies assisted the ice formation by keeping the discharges around 200–300 m^3s^{-1}. The upstream boundary condition was taken as the daily discharge from the Harjavalta power plant. Every 15 minutes, water level records from the W1 station were used as the lower boundary condition.

Unsteady simulations were carried out with constant ice cover thicknesses and with two n_i-values (Figure 5). The simulations with smooth 10 or 20 cm-thick ice covers can be considered most representative for the actual prevailing situation. A 30 thick and smooth ice cover as an input into the HEC-RAS simulation produce slightly too high water levels (Figure 5). Considering that the period represents the beginning of the ice formation, and the temperature was clearly below zero for the whole period, it can be taken as encouraging that the 10 cm ice thickness applies best in the beginning of the simulation, and 20 cm thickness in the latter period 23–30 January (Figure 5). According to verification, the n_i-value 0.03 is too large to be applied in the freezing phase, when the ice cover is thickening. As a whole, the simulations performed satisfactorily and the model can be considered to describe well the hydro-dynamic system of the river, and the actual projections can be considered reliable for simulating impacts of climate change scenarios.

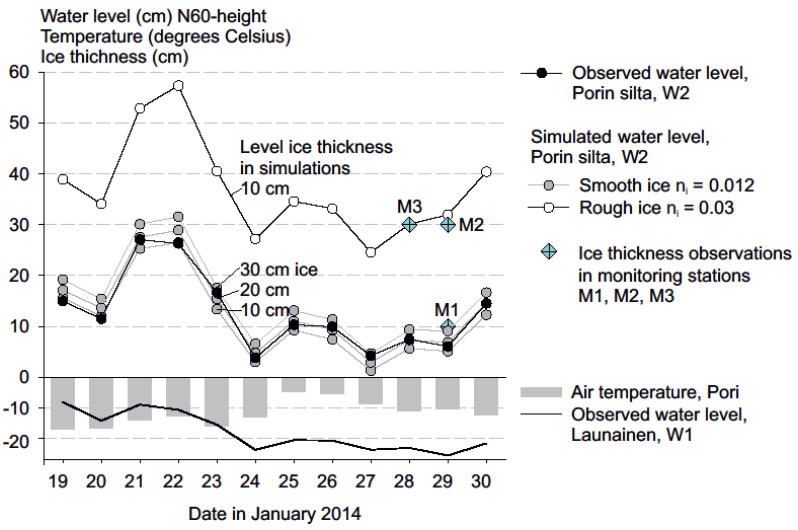

Figure 5. Daily mean observed and simulated water level at the Pori Bridge monitoring station during 19–30 January 2014. The air temperature was measured in Pori (©Finnish Meteorological Institute)

4. RESULTS

4.1 Turbidity variations along a river stretch

To detect possible bed erosion of a 15 km long river stretch, we analysed turbidity data collected from monitoring sites, M1 and M5, during the same days. The monthly mean turbidity was in the upstream 8–52 FNU, and in the downstream site 9–54 FNU (Figure 6). The evidently high turbidity of July represents a single measurement day, since the station M1 was sampled only once in July. The turbidities in M1 and M5 were, however, consistent for that single sampling date. The M5 station was sampled more frequently, and the average turbidity for July was 11 FNU (N = 34), which is in line with the mean turbidity observed in the other summer months.

During January–March, when the river is usually ice-covered, the turbidity was on average only 0.6 FNU higher in the downstream than in the upstream location. The rest of the year, the mean difference was 1.3 FNU. The most pronounced difference between the sites was during April and May, showing a difference of 2.1 FNU. In conclusion, the difference of observed turbidities is small but consistent, suggesting a net erosion process for the river stretch in combination with other phenomena like a contribution from the surrounding watershed. The actual magnitude of each contributing process cannot be distinguished with the data available.

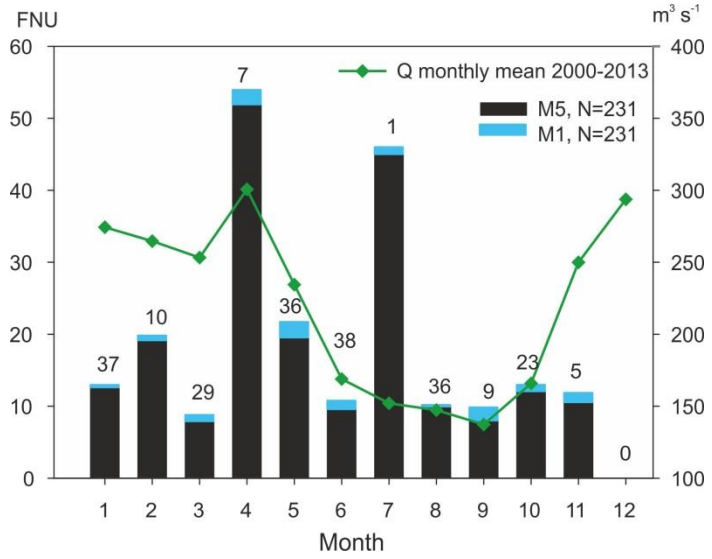

Figure 6. Monthly mean turbidity during 1975–2013 and discharge during 2000–2013 in sites M1 and M5. The numbers on top of the bars indicate the number of days when turbidity water samples were taken from both measurement sites. FNU, Formazin Nephelometric Unit

4.2 River ice cover influence on turbidity

The impact of the ice cover on the turbidity is illustrated in the Figure 7. With a low discharge (< 100 m^3s^{-1}), the mean turbidity of the ice-covered river flow was only about one third of the turbidity of the summer or autumn flow. With discharges between 100–300 m^3s^{-1}, the turbidities of ice cover periods were still markedly lower than ice-free periods, the difference being highest between ice cover and autumn periods. The discharge category 200-300 m3/s covers the mean winter discharge. In this category the mean turbidity of ice-covered river flow is 50 % of the winter ice–free river.

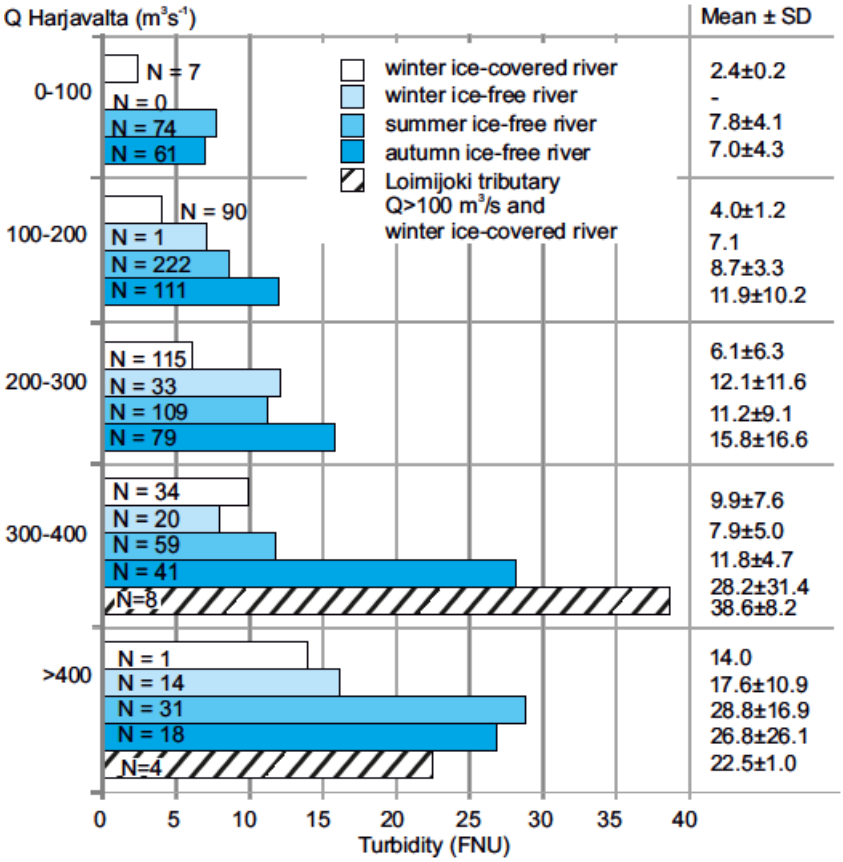

Figure 7. Mean turbidity and its standard deviation in ice-covered flow and ice-free flow, according to seasons in five different discharge categories during 1973–2013. N denotes the number of observations

The Student's t-test was conducted to test if the mean turbidity of the ice-covered river water differentiates from the turbidity of the summertime ice-free flow within the discharge range 100–200 m^3s^{-1}. Within these two groups the number of observations was large enough and the standard deviation of the datasets was small compared to the means (Figure 7). There was a significant difference between the ice-covered period turbidities and the summertime turbidities; $t(308) = -18.2$, $p = 0.00$. This result suggests that an ice cover really does have a diminishing effect on turbidity up to −54 %, compared with the open water river, since washload during summer is low due to high evapotranspiration. The lack of observations hindered the finding of any statistically significant conclusions about ice effect on turbidity when $Q < 100$ m^3s^{-1} or when $Q > 300$ m^3s^{-1}.

High discharge (> 300 $m^{-3}s^{-1}$) events are rare in ice-covered Kokemäenjoki River. Winter high discharges are usually connected to ice clearance period when the river is partly ice-covered and partly in an open-flow condition e.g. the Raumanjuopa distributary is still ice covered while the main channel is already ice-free. In high discharges, the river regulation and highly turbid water from Loimijoki tributary are the main explanations for increased turbidities during winter ice cover periods (Figure 7). The mean discharge 23 m^3s^{-1} (1971–2013) of the Loimijoki tributary is 9 % of the average discharge of the Kokemäenjoki River. During high discharge events, the hydropower companies store as much as possible of the water in the upstream reservoirs. Concurrently, the discharge in the highly turbid Loimijoki River increases by relatively much more than the discharge in the main channel. The mean turbidity in the ice-covered river water (Q = 300–400 m^3s^{-1}) is only 9.9 FNU (N=34) in cases where the Loimijoki River discharge has been below 100 m^3s^{-1} – comprising 5 % of the discharge in Harjavalta – and as high as 38.6FNU (N=8) if the Loimijoki River discharge has been above 100 m^3s^{-1}, i.e. 20-40 % of the Harjavalta discharge. The turbidities measured in the ice-free river present a situation when the Loimijoki tributary discharge is less than 20 % of the Harjavalta discharge.

4.3 Temporal variation of river sediment load

The inter-annual, seasonal, and monthly riverine sediment load are highly varying due to hydro-climatic conditions like in many northern rivers (Woo and McCann 1994). The estimate of mean annual load of suspended solids into the Baltic Sea from the Kokemäenjoki River was 120 000–150 000 tonnes during 1990–2013, based on both VEMALA simulations and observations, i.e. observed monthly averaged discharges and available TSS data. The annual minimum and maximum loads were 43 000 and over 200 000 tonnes respectively.

The three winter months, Dec—Feb, comprise approximately 26 % of the annual TSS load based on the VEMALA simulations (Figure 8). The spring freshet is presently the most significant period of riverine sediment load. April alone comprises 21 % of the annual TSS load of the Kokemäenjoki River. Part of the springtime riverine TSS load originates from the watershed, as over half of the annual runoff takes place during the spring in southern Finland. The discharges and runoff are low during summer, which is reflected in sediment loads. At the end of the year, a peak in the sediment load is typical due to increasing precipitation and discharge.

4.4 Climate change effects on hydro-meteorology

The projected climate change is reflected in hydro-meteorological parameters like temperature and precipitation, and in future discharges of the River Kokemäenjoki (Table 1). Hydrological model simulations with five climate scenarios indicate changes in the annual cycle of discharges. In the winter months, Dec–Feb, the discharge will increase during the period 2010–2039 (Table 1). By the period 2070–2099 the mean winter discharges are projected to be 27–77 % larger than during the control period 1971–2000. In contrast, the projected annual mean discharges may decrease by 13 % or increase by 42 %, depending on the climate scenario (Table 1). HadCM3-RCA3 indicates that the summer discharges would prevail at the present level or slightly increase, but the other scenarios predict that the mean summer discharges will decrease (Figure 9). Three climate scenarios (Table 1 and Figure 9) presenting the projected winter average and winter extremes are selected for future load estimates (Section 4.5) and hydrodynamic shear stress simulations (Section 4.6).

A warmer climate will cause more snow melting and diminish the snow water equivalent in Finland (Vehviläinen and Huttunen 1997).The climate models project on average a 0.1˚C mean winter temperature for Pori during 2070–99, which indicates a temperature increase of 4.6 degrees compared to the −4.5˚C of the control period. The increasing rainfall and snow melt will increase winter discharges.

The sea level height has an influence on river water levels in the lower reach of the Kokemäenjoki River. Johansson et al. (2014) indicated that the relative sea level change on Mäntyluoto (Figure 1) will be on average −13 cm from 2000 to 2100, since the land uplift rate 8.5 mm/yr is stronger than the projected sea level rise. According to this medium scenario, the average of the Mäntyluoto sea level will be −0.32 m (N60) in 2100, which is presumed to be the most likely scenario. We also simulated the shear stress variation according to the low and high sea level scenarios −0.76 m (N60) and +0.24 m (N60) respectively.

4.5 Climate change effects on seasonal riverine sediment load distribution

Estimates of future changes in seasonal riverine sediment loads were calculated based on equations 1 and 2 and on three climate change scenarios. The control in Figure 10 presents an estimate of the monthly loads when the river is ice-covered during Jan–March. The GLOB and HadCM3-RCA3 scenarios, project clear increasing trends for the annual discharges, which in turn will be reflected in increasing amounts of annual riverine sediment loads. GLOB and HadCM3-RCA3 project a 10 % and 70 % increase to the annual sediment loads respectively, compared with the control run if ice cover exists in the river. ARPEGE-HIRHAM indicates a decreasing trend for the annual discharge, leading to a −25 % decrease of annual sediment load. For the case in which ice cover does not form at all, the three scenarios project 10–120 % increase in the annual loads.

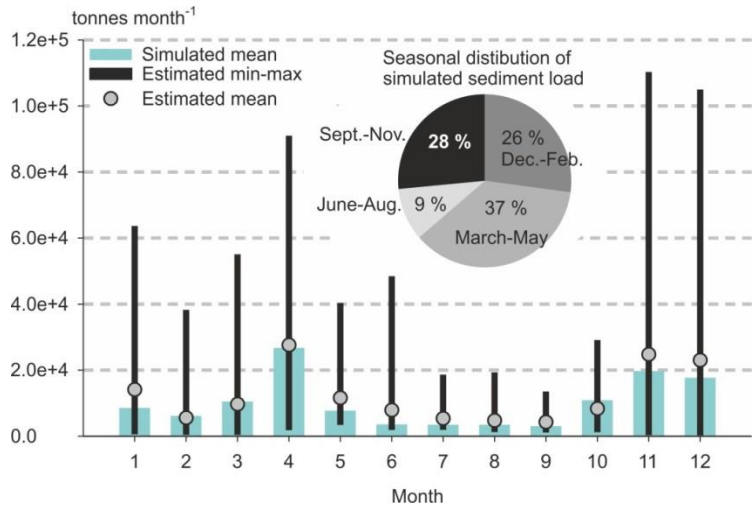

Figure 8. Simulated and estimated suspended solid load based on observations from the river Kokemäenjoki to the Pihlavanlahti estuary during 1990–2013. The estimated monthly loads are calculated from observed monthly mean discharges and observed total suspended solids concentrations, N =313

Table 1. The projected mean annual and winter (December–February) discharges of the Kokemäenjoki River in Harjavalta, as well as mean winter temperature and precipitation in Pori together with data of control period 1971–2000

Simulation/Observation	**Q_{annual}** [m^3s^{-1}]			**Q_{winter}** [m^3s^{-1}]			**T_{winter}** [C°]	**P_{winter}** [mmd^{-1}]
Control run 1971–2000	230			256			–4.5	1.6
Observation 1971–2013	231			260				
Climate scenario	2010–2039	2040–2069	2070–2099	2010–2039	2040–2069	2070–2099	2070–2099	2070–2099
ARPEGE–HIRHAM	253	202	199	355	314	326*)	−0.9	1.6
HadCM3–HadRM	216	219	225	320	355	393	−0.1	1.9
GLOB, 19 global climate models	232	244	252	323	368	407*)	1.1	1.9
HadCM3–RCA3	269	302	326	352	404	454*)	0.5	1.9
ECHAM5–RCA3	236	247	267	277	309	395	−0.3	2.0
Mean of the five scenarios	241	243	254	325	350	395	0.1	1.9

*) scenario selected for future sediment load projections and hydrodynamic shear stress simulations

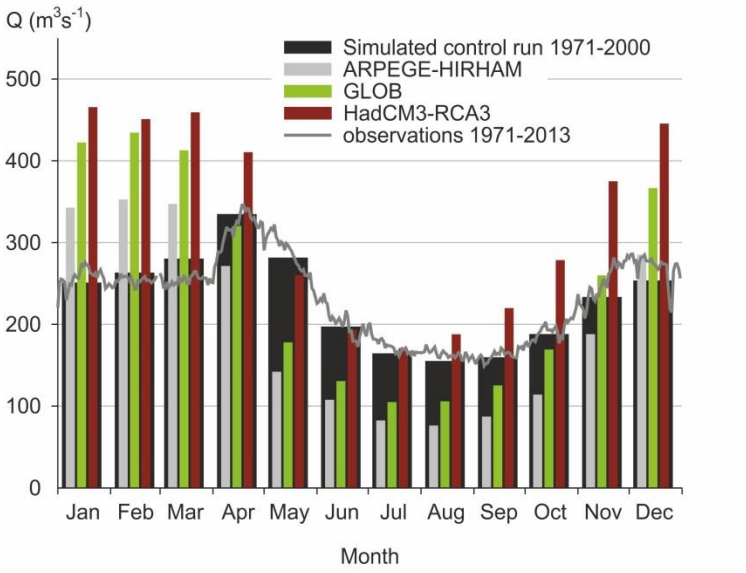

Figure 9. Simulated monthly discharges in the Harjavalta Dam for the period 2070–2099 with three climate scenarios, control period 1971–2000 and observed daily mean discharges for 1971–2013

The annual riverine sediment load will be redistributed within the seasons due to the climate change. In the future, the period December–March will comprise a larger percentage of the annual load. The percentage is dependent on the ice cover duration and climate scenario. According to scenarios, 40–50% of the annual load will take place during December–March (control run 25 %) if the ice cover period lasts three months. The percentage of the control run is 40 % and scenarios 50–70 % if the river stays ice-free during the whole winter.

During Jan–March, all three scenarios ARPEGE-HIRHAM, GLOB and HadCM3-RCA3 project an increase in sediment loads by 60, 140 or 180 % respectively in the case that the river is also ice-covered in the future. The importance of the river ice cover in controlling the amounts of wintertime sediment loads is evident, since if the river stays ice-free during the whole winter, the projected increase of wintertime sediment loads is 300–500 % (Figure 10). The results indicate that during the ice season (Jan–March), the sediment load may double from the present level by 2070–99 due to increasing discharge. For the case in which the ice cover periods shorten, the increase in wintertime riverine sediment loads is even higher.

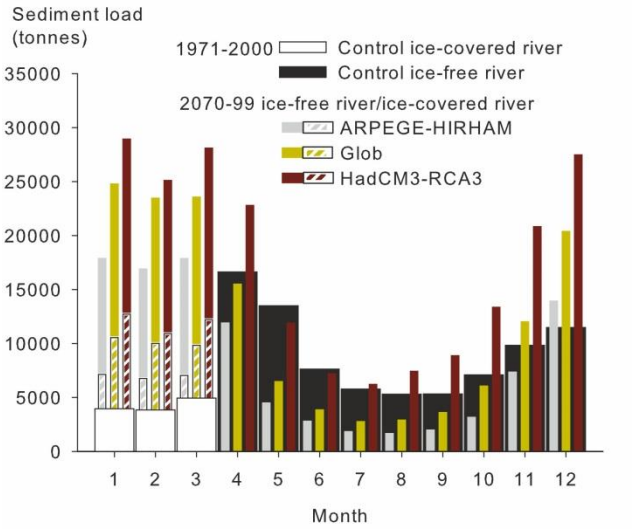

Figure 10. The future change of seasonal sediment load distribution and influence of river ice cover on monthly sediment loads. Load estimates are based on simulated monthly discharges of the control period 1971–2000 versus climate scenarios for 2070–2099. The striped bars indicate estimates when an ice cover exists on the river

4.6 Shear stress variation due to ice in present and future hydro-climatic states

The mean shear stress in each cross section of the study reach was simulated with HEC-RAS, for present and for 2070–2099 projected boundary conditions (Table 2). The results suggest that a smooth thermally formed ice cover diminishes the shear stress compared with open water flow (Table 3). With the present mean winter discharge, a smooth and 5–40 cm-thick ice cover reduces the average τ in each cross section, compared with open water flow (Figure 11). The average reduction of τ is 29–36 % depending on the ice cover thickness. In contrast, rough ice cover increases or decreases simulated τ compared with open water flow, depending on channel geometry (Figure 11), since the mean shear stress decreases by −1 % or increases by 7 % (Table 3).

Table 2. Boundary and ice conditions used in hydrodynamic shear stress simulations

Present hydro-climatic conditions		**Climate scenarios**			
Upstream boundary	Downstream boundary	Upstream boundary	Downstream boundary, W1 Water level 2100 (m) N60-height		
			Low sea level	Medium sea level	High sea level
260 m^3s^{-1} Harjavalta $Q_{winter,\ Dec.-Feb.}$ 1971–2013	+0.0 m (N60) Launainen (W1) mean observed winter time (Dec.-Feb.) water level	Q = 326 m^3s^{-1} ARPEGE-HIRHAM	−0.54	−0.10	+0.46
		Q= 407 m^3s^{-1} GLOB	−0.48	−0.04	+0.52
		Q = 454 m^3s^{-1} HadCM3-RCA3	−0.44	−0.01	+0.56
Ice conditions					
Open water					
Ice cover extent: Pihlavanlahti Bay-Harjavalta Dam					
Ice thickness 5-40 cm					
Ice roughness, Manning's n: 0.012 or 0.03					

Independent of the discharge, the smooth ice reduces the erosion potential throughout the simulated river stretch (Figures 11–12). The high shear stress peak visible at point 33 km upstream from the estuary (Figure 12) is due to rapids. For rough ice, however, there are sections in the lower part of the simulated river stretch (0–21 km) – both at present and for projected future conditions – where the erosion potential either increases or reduces compared with the open water conditions. Instead, for the upper river stretch (21–39 km), the rough ice reduces the erosion potential (Figures 11–12). This effect was similar in all simulated discharge scenarios. The variation of ice influence on shear stress is explained by the variation in the channel geometry and dimensions of the cross sections. Rough ice reduces the conveyance of the channel more in the lower part of the simulated river stretch than in the upper stretch.

Table 3. Simulated shear stress of the ice-covered and ice-free Kokemäenjoki River stretch 0–30 km in case of observed mean winter discharge 1971–2013 and projected discharges 2070–2099: ARPEGE-HIRHAM, GLOB, HadCM3-RCA3, and the mean sea level scenario for year 2100

	Open water				**Smooth ice cover, n = 0.012**								**Rough ice cover, n = 0.03**							
Ice thickness (cm)	0	0	0	0	5	5	5	5	40	40	40	40	5	5	5	5	40	40	40	40
Q (m^3s^{-1})	**260**[1)]	326[2)]	407[3)]	454[4)]	**260**[1)]	326[2)]	407[3)]	454[4)]	**260**[1)]	326[2)]	407[3)]	454[4)]	**260**[1)]	326[2)]	407[3)]	454[4)]	**260**[1)]	326[2)]	407[3)]	454[4)]
Shear stress (Nm^{-2})																				
Mean	**1.34**	1.84	2.46	2.81	**0.85**	1.20	1.58	1.80	**0.95**	1.31	1.69	1.91	**1.32**	1.81	2.33	2.64	**1.43**	1.92	2.45	2.76
Std.Dev.	**0.80**	1.03	1.29	1.44	**0.45**	0.57	0.70	0.77	**0.48**	0.60	0.71	0.77	**0.55**	0.68	0.80	0.87	**0.57**	0.68	0.80	0.87
Min	**0.17**	0.26	0.38	0.46	**0.13**	0.21	0.29	0.34	**0.14**	0.21	0.30	0.35	**0.22**	0.32	0.44	0.52	**0.23**	0.32	0.44	0.52
Median	**1.11**	1.50	2.06	2.36	**0.78**	1.10	1.50	1.69	**0.85**	1.18	1.60	1.79	**1.30**	1.72	2.22	2.54	**1.41**	1.85	2.37	2.67
Max	**4.17**	4.83	5.52	6.17	**2.19**	2.57	3.15	3.55	**2.37**	2.70	3.33	3.68	**2.52**	3.31	4.19	4.68	**2.62**	3.39	4.26	4.75

The projected increases in winter discharge by 2070–99 lead to an increase of winter period shear stresses (Table 3 and Figures 12) when we compare the open water simulations with present discharge to the projected ones. In the cases of smooth and 5–40 cm-thick ice cover simulations, the mean wintertime shear stress is projected to increase from the present range of 0.9–1.0 Nm^{-2} to 1.2–1.9 Nm^{-2}. In the case of rough ice cover with thickness 5–40 cm, the mean wintertime τ is projected to increase from the present range of 1.3–1.4 Nm^{-2} to 1.8–2.8 Nm^{-2}. For an ice-free river in the future, the mean shear stress would be even larger (Table 3). The τ_{crit} values 1.4–6.1 Nm^{-2} (Lotsari *et al.*, 2014) will be exceeded more often in the future. The results in Figures 12 are based on ARPEGE-HIRHAM projected discharges and the medium sea level scenario. The lower sea level heights would increase the projected shear stresses of the simulated river stretch by approximately 10 %, due to increasing S_e, and the high sea level rise scenario would decrease τ approximately 10 % compared to the medium sea level scenario. Actually, the sea level scenarios have an effect on τ only in the stretch 0–20 km. Upstream from there, the river bed elevation is so high that the sea level influence becomes insignificant.

The longitudinal shear stress variation calculated according to the ARPEGE-HIRHAM climate scenario projects the least changes in hydrology (Figure 12). The longitudinal changes in average shear stress with GLOB or HadCM-RCA3 projected discharges are similar to those in Figure 12 the only difference being that the shear stress levels are higher due to larger discharges. The future wintertime τ will face an overall increase if we compare it to the τ with present winter discharge and 5 cm-thick smooth ice conditions. The increase in the future τ is the largest with the HadCM3-RCA3 scenario, which also projects the largest increase in annual and winter discharges together with the most intensive warming.

5. DISCUSSION

5.1 Ice cover influence on sediment processes

The turbidity, TSS and shear stress analyses indicate that the sediment transportation in the river declines under ice cover. Findings from laboratory studies (Sayre and Song, 1979; Lau and Krishnappan, 1985; Ettema *et al.*, 2000; Muste *et al.*, 2000) conclude the same effect. According to hydrodynamic simulations, a smooth ice cover that is vertically responding to water level changes decreases the average shear stress relative to open water flow with similar discharges. A reduction was indicated throughout all simulated ice cover thicknesses. Thus, the reduction is declining when the ice cover is thickening. According to Ettema and Kempema (2013) level ice cover elevate flow depths, and thereby decreases flow velocities as well as sediment transportation rates, which is in line with our smooth ice cover simulations. More detailed information of ice effects on shear stress variations in a reach and cross-section scale could be

achieved by applying a 1-D or 2-D hydrodynamic model (Knack *et al.,* 2010) together with an river ice growth and decay model.

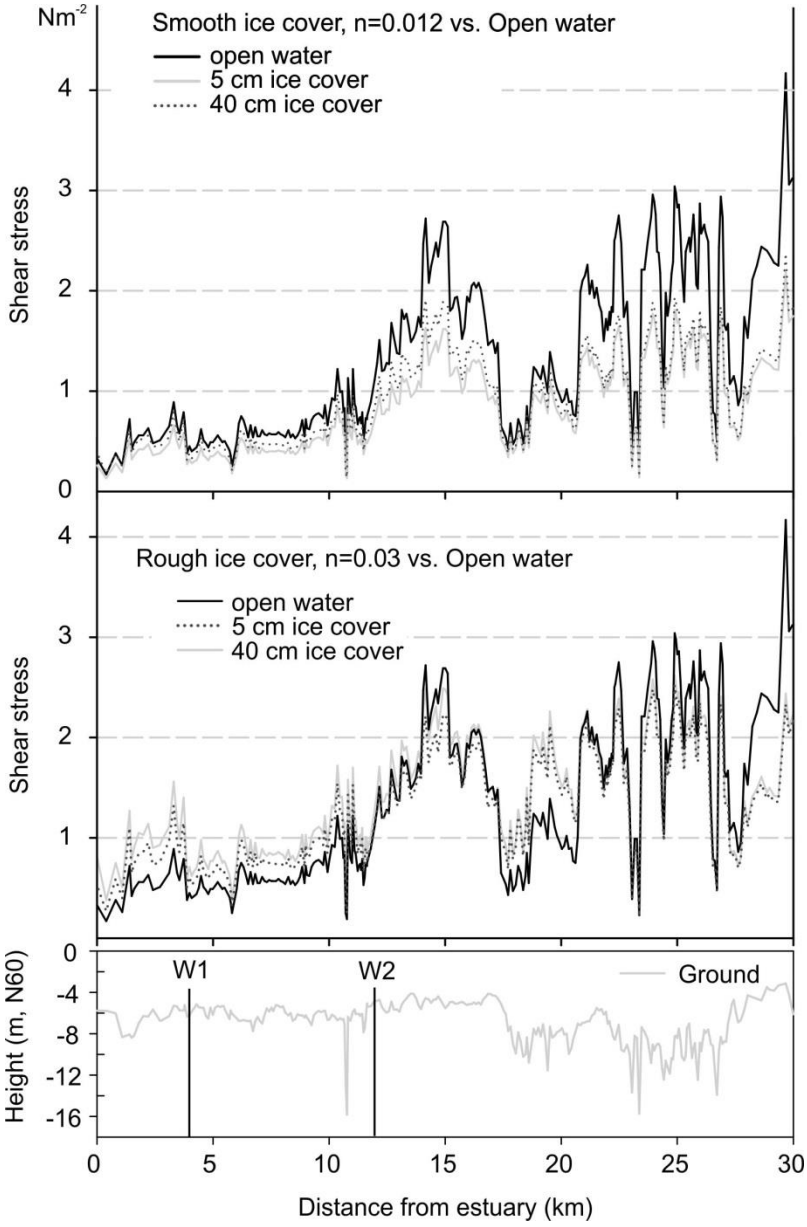

Figure 11. Simulated shear stress variation in the longitudinal profile of the Kokemäenjoki River for ice-covered and open flow river, together with the mean winter discharge, Q = 260 m^3s^{-1}. The river bed elevation and water level observation sites W1 and W2 are indicated at the bottom

The laboratory results of Muste et al. (2000) indicated that TSS load decreases with the increase of cover roughness. In contrast, our simulations suggest that a

rough ice cover increases or decreases the shear stress depending on the river slope and the variation of channel cross-section shapes and roughness. Parts of the cross sections faced a more intense decrease in conveyance of the channel together with a pronounced increase of S_e due to rough ice cover. Thereby, it resulted in local increases of river bed erosion potential. Ice cover of a given thickness has a greater effect on flow characteristics the more area it occupies of the channel cross section (Ettema and Kempema, 2013).

Comparison of the turbidities at two measurement points indicated channel bed erosion. The result is in line with the study by Lotsari et al. (2014) showing that net erosion is dominant in that stretch of the Kokemäenjoki River. The turbidity data also indicated less river bed erosion during ice-covered months than in the rest of the year. Ettema and Kempema (2013) state that ice usually reduces the channel's capacity to convey the eroded sediment a significant distance from the erosion location, but that issue was not possible to analyse within this study.

The analysis of winter and summertime turbidities suggest a statistically significant diminishing effect of ice cover on river turbidity. The observed reduction in turbidity due to ice cover is in the range of 30–70 % during low discharges ($Q<300$ m^3s^{-1}). Lau and Krishnappan (1985) have determined in a laboratory that a floating top cover reduces the sediment transport rate by 61–74 %, i.e. to about one-third of the corresponding free-surface flow. Ice cover as a diminishing factor in river sediment transportation should not be underestimated since it´s importance can be quite significant depending on the variation of ice cover duration.

Kinematic viscosity increases when water is cooling. Increasing viscosity may increase suspended sediment transport in certain conditions depending on sediment type and flow magnitude (Akalin 2002, Hong 1984, Taylor, 1971). In our data a clear tendency is not observed that the wintertime water turbidities would be higher than during summer.

The autumn turbidities are often higher than during summer. These reflect mainly sediment washload from the watershed, since a considerable part of erosion of arable areas occurs in autumn in SW Finland (Puustinen *et al.*, 2007). During the high discharge events ($Q> 300$ m^3s^{-1}) in particular, the fine sediment originating from the unfrozen watershed increases the river sediment load. During the summer, the washload is of minor importance due to large evapotranspiration (Puustinen *et al.*, 2007), low runoff and dry soils. Also, during river ice and snow covered periods, the washload is at minimum.

A few issues should be noted in relation to representativeness of turbidity data. The instantaneous turbidity samples were bound to the daily average discharges. Those absolutely do not always reflect the turbidity induced by the daily mean discharge. In the regulated river, the short-term discharge variation – especially in wintertime – may be large due to hydropeaking. This may partly explain the large standard deviations of the turbidity data in respect to discharges. A more comprehensive study on ice influence on turbidity could be conducted by collecting a coherent time series of river turbidity and discharge variation, covering both ice

cover and summer seasons. Acoustic sensors developed to continuously monitor water turbidity, even beneath an ice cover, have been applied in a few studies (Linjama *et al.*, 2009; Koskiaho *et al.*, 2010; Moore *et al.*, 2013; Weiss, 2013).

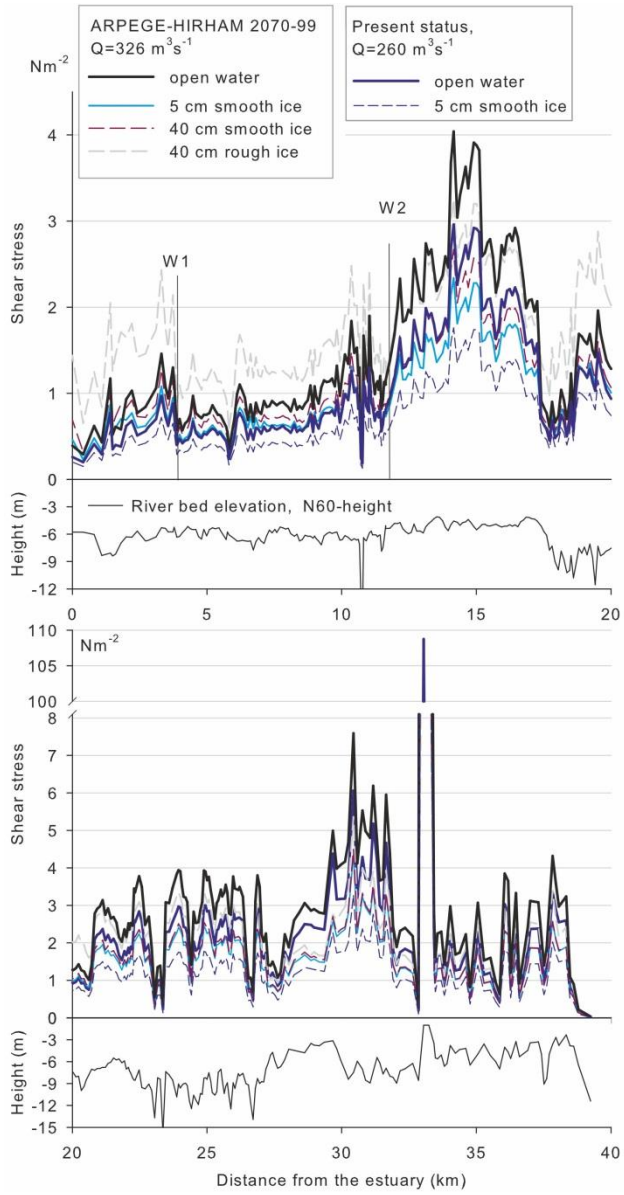

Figure 12. Longitudinal changes in average shear stress in open water and ice conditions with ARPEGE-HIRHAM projected discharge for 2070–2099 and the medium sea level scenario. Two simulated shear stress variations with present winter discharge are also presented. For water level station locations W1 and W2, see Figure 1

5.2 Future scenarios 2070–2099

The climate scenarios do not provide a coherent signal in respect of future annual mean discharges (Table 1). Thus, the sources of uncertainties connected to future trend of annual loads are large starting from climate scenarios. Instead, prominent and coherent changes are expected in the seasonal distribution of river discharges and riverine sediment loads according to each climate scenario. Wintertime discharges and riverine sediment loads are evidently increasing. In the future, the Dec.–March periods will contribute 40–70 % of the annual sediment load, which is clearly more compared with the control runs 25–40 %.

For typical ice cover months January-March, the riverine mean loads may double due to the increasing winter discharges of the GLOB scenario. Shortening ice cover periods are projected (Prowse *et al.*, 2011) and he load increase is most pronounced in an extreme scenario if the river stays ice-free the whole winter. In that case, sediment load during the three winter months would almost triple compared with the control run, when the discharges of the GLOB scenario are applied. Futhermore, in winters with frost-free soil and little snow, the risk of increased erosion of arable land will inevitably increase during mild and rainy winters (Puustinen *et al.*, 2007). The summertime sediment loads will diminish according to the GLOB scenario. Instead, HadCM3-RCA3 projects such high discharges that during summer, the sediment loads would also increase as we compare those with control runs.

The under-ice period is a time of fine-grained sediment deposition (Milburn and Prowse, 1998). This sediment deposition resuspends just before river-ice breakup (Milburn and Prowse, 2002). Presently, the highest TSS concentrations and an intensive sediment load peak are accompanied by freshet in April in the Kokemäenjoki River. Potential open water periods and larger discharges during winters in the future would also redistribute the transportation of fine-grained material to take place occasionally during the whole winter, rather than being concentrated to the short freshet.

The projected winter mean shear stresses for 2070–2099 will increase from the present level, due to higher discharges. The increase of τ and erosion potential of the river bed will be enhanced by shorter ice cover periods. A straightforward thinking is that river ice cover periods are shrinking and the ice thicknesses will decrease in cold regions in the future. However, annual and monthly variations will still exist and, based on this study, we are not able to predict the future behaviour of the ice covers. There is also evidence that in certain conditions, solid-ice thickness has increased despite a concomitant rise in winter temperature (Beltaos, 2008). Moreover, uncounted factors will affect the future riverine sediment loads. The Kokemäenjoki River is regulated for power supply purposes. Water level and discharge fluctuations due to hydropeaking can affect turbidity and the riverbed morphology (Huttula and Krogerus, 1986; Charmasson and Zinke, 2011). Those are not comprehensively analysed in this study.

Sources of uncertainties in winter sediment load projections are largely related to variation in future discharge approximations, correlation of sediment loads with discharges, length of river ice cover periods, and sediment concentrations of run-off water from catchment areas. Woo and MacCann (1994) have also recognized the large variability of uncertainties in estimation of sediment loads. The variation should be taken into account when interpreting the estimated loads. In the future mid-winter thaws followed by cold spells may become more common and favor frazil formation (Huokuna *et al*. 2009). Anyhow, anchor ice is more important contributor to direct ice entrainment and transport of bed material than frazil ice (Ettema and Kempema 2012). Anchor ice usually occurs in gravel bed rivers (Kempema and Ettema 2011), but not in fine sediment rivers like the Kokemäenjoki River.

However, according to our case study, it is evident that both the erosion potential of the river bed and the sediment yield of the receiving water body will increase during winters. The temporal variation of riverine sediment loads is large and the seasonal variations will be even larger in the future. The combined effects of climate change on the riverine sediment loading are thus superimposed on the effects of river ice and other natural factors. The single effect of each individual factor remains still to be more thoroughly quantified.

CONCLUSIONS

The study provided an insight on the ice cover effects on sediment processes in a medium-size river characterized by fine sediments. Long-term monitoring data of river ice and turbidity enabled us to draw a statistically significant conclusion that river ice is decreasing the river bed erosion. In addition, the future trends and seasonal variation in riverine sediment loads up to 2070–99 are outlined. The following conclusions can be presented:

- The mean turbidities of ice-covered river water were observed to be 1.5–3.3 times smaller than in ice-free situations during summer or winter with similar discharges ($Q<300$ m^3s^{-1}).
- The turbidity observations from two river monitoring sites (M1 and M5) indicate that bed erosion decreases during ice-covered periods.
- In general, the effect of ice cover on shear stress is dependent on channel characteristics and ice cover thickness and roughness. According to turbidity observations and shear stress simulations, the net effect of ice cover in the studied river has been to reduce the shear stress compared with the open water state.
- The trend of increasing winter discharges of the Kokemäenjoki River is coherent when based on each climate scenario. However, the annual

discharges are projected to increase or decrease depending on the climate scenario.

- The annual riverine sediment load will be redistributed within the seasons, due to the climate change. In the future, the period December–March will comprise a larger percentage of the annual load. The percentage is dependent on the ice cover duration and climate scenario. 40–50 % of the annual load will take place during December–March if the ice cover period lasts three months. The percentage is 50–70 % if the river stays ice-free during the whole winter.
- The riverine sediment loads during winters are expected to double due to increased discharges by 2070–99. It is possible that shortening the ice cover periods would still increase the river bed erosion and sediment loads.

The present study is one of the very few available studies attempting to quantify the effects of river ice cover on sediment processes in a natural river (Ettema and Kempema 2012, Lawson *et al.* 1986), i.e. not a laboratory channel. We were able to recognize significant effects of river ice on sediment processes. Possible future scenarios of sediment loads in ice-covered and ice-free rivers were also outlined. These should be interpreted as indicative. The present and future riverine load estimates could be enhanced by arranging, e.g., a year-long continuous monitoring campaign of key parameters.

ACKNOWLEDGEMENTS

This work was supported by the Academy of Finland [grant number 267345 (ExRIVER)]; [grant number 136234 (RivCHANGE)]; the Maj and Tor Nessling Foundation [grant number 201300067 (ExRIVER)]; Ministry of Agriculture and Forestry [grant number 311290 (LuhaGeoIT)].

REFERENCES

Aaltonen J. 2006. Porin tulvat -hankkeen osaselvitys: Avotilan virtauslaskenta ja tulvakarttojen laatiminen. In *Porin tulvat -hanke 2003-2006*, Loppuraportti CD, Suomen ympäristökeskus.

Akalin, S., 2002. Water temperature effect on sand transport by size fraction in the Lower Mississippi River. Ph.D. thesis. Colorado State University, Fort Collins, USA; 218 pp.Beltaos S. 1995. *River Ice Jams*. Water Resources Publications: Colorado; 372

Beltaos S. 2008. Hydro-climatic impacts on the ice cover of the lower Peace River. *Hydrological Processes* **22**: 3252-3263. DOI: 10.1002/hyp.6911.

Beltaos S, Prowse T. 2009. River-ice hydrology in a shrinking cryosphere. *Hydrological Processes* **23**: 122–144. DOI: 10.1002/hyp.7165.

Bergström S. 1976. *Development and Application of a Conseptual runoff model for Scandinavian Catchments*. Swedish Meteorological and hydrological Institute, Report RHO No. 7: Norrköping; 134 pp.

Boucher E, Bégin Y, Arseneault D, Ouarda TBMJ. 2012. Long-Term and Large-Scale River-Ice Processes in Cold-Region Watersheds. In *Gravel-Bed Rivers: Processes, Tools, Environments*, Church M, Biron PM, Roy AG (eds). John Wiley & Sons Ltd: Chichester; 546–554.

Brunner WG. 2010. *HEC-RAS, River Analysis System Hydraulic Reference Manual*. US Army Corps of Engineers Hydrologic Engineering Center (HEC), Report CPD-69: Davis CA; 411 pp.

Carey KL. 1966. Observed configuration and computed roughness of the underside of river ice, St. Crois river Wisconsin. In *Geological Survey research 1966, Chapter B*. U.S Geological Survey Professional Paper 550-B: Washington; B192-B198.

Carey KL. 1967. The underside of river ice, St. Crois River, Wisconsin. In: *Geological Survey research, Chapter C*. U.S. Geological Survey Professional Paper, 575-C: Washington; C195- C199.

Charmasson J, Zinke P. 2011. *Mittigation Measures Against Hydropeaking Effects*. SINTEF Report TR A7192: Trondheim; 51 pp.

Chow VT. 1959. *Open channel hydraulics*. McGraw-Hill book company: New York; 680.

Cripps C, Peltonen J, Räsänen M, Huhta P, Niinikoski J. 2011. *Development of the river Kokemäki delta, its Quaternary sediments and their chemical characteristics*. Centre for Economic Development, Transport and the Environment for Southwest Finland Publications 13/2011 (in Finnish): Jyväskylä; 61 pp.

Drebs A, Nordlund A, Karlsson P, Helminen J, Rissanen P. 2002. *Tilastoja Suomen ilmastosta 1971-2000 - Climatological Statistics of Finland 1971-2000*. Finnish Meteorological Institute: Helsinki; 94 pp.

Ettema R, Braileanu F, Muste M. 2000. Method for estimating sediment transport in ice-covered channels. *Journal of cold regions engineering* **14**: 130–144. DOI: 10.1061/(ASCE)0887-381X(2000)14:3(130).

Ettema R, Daly SF. 2004. *Sediment transport under ice.* Cold Regions Research and Engineering Laboratory U.S. Army Engineer Research and Development Center ERDC/CRREL TR-04-20: Hanover, NH; 54 pp.

Ettema R, Kempema EW. 2012. River-Ice Effects on Gravel-Bed Channels. In *Gravel bed rivers: processes, tools, environments*, Church M, Biron PM, Roy AG (eds) John Wiley & Sons Ltd: Chichester; 525–540.

Ettema R, Kempema EW. 2013. Ice effects on sediment transport. In *River Ice Formation*, Beltaos S (ed.) Committee on River Ice Processes and the Environment, Canadian Geophysical Union Hydrology Section: Edmonton; 297-338.

Hassanzadeh Y. 2012. Hydraulics of Sediment Transport. In *Hydrodynamics - Theory and Model*, Zheng J-H (ed.) InTech: 23-59 DOI: 10.5772/25982.

Hay LE, Clark MP, Wilby RL, Gutowski WJ, Leavesley GH, Pan Z, Arritt RW, Takle ES. 2002. Use of regional climate model output for hydrologic simulations. *Journal of Hydrometeorology* **3**: 571–590. DOI: 10.1175/1525-7541(2002)003<0571:UORCMO>2.0.CO;2

HELCOM. 2010. *Ecosystem Health of the Baltic Sea 2003-2007: HELCOM Initial Holistic Assessment*. Helsinki Commission, Baltic Sea Environment Proceedings No. 122: Helsinki; 63 pp.

Hong R-J. 1984. Low-Temperature Effects on Flow in Sand-Bed Streams. *Journal of hydraulic Engineering* **110**: 109–125. DOI: 10.1061/(ASCE)0733-9429(1984)110:2(109)

Huokuna M. 2007. Ice Jams in Pori. In *Proceedings of the 14th Workshop of the Committee on River Ice Processes and the Environment*: Quebec City.

Huokuna M, Aaltonen J, Veijalainen N. 2009. Frazil ice problems in changing climate conditions. In *Proceedings of the 15th Workshop on River Ice*, St. John´s, NF; 118–126.

Huttula T, Krogerus K. 1986. Water currents and erosion of cellulose fibers in short term regulated water cource. *Aqua Fennica* **16**: 167–180.

Huttunen I, Huttunen M, Seppänen V, Korppoo M, Lepistö A, Räike A, Tattari S, Vehviläinen B. submitted. A national scale nutrient loading model for Finnish watersheds - VEMALA. Submitted to *Environmental Modeling and Assessment*.

Johansson MM, Pellikka H, Kahma KK, Ruosteenoja K. 2014. Global sea level rise scenarios adapted to the Finnish coast. *Journal of Marine Systems*, **129**: 35-46. DOI: 10.1016/j.jmarsys.2012.08.007.

Kempema EW, Ettema R. 2011. Anchor ice rafting: Observations from the Laramie River. *River Research and Applications* **27,** 1535–1467. DOI: 10.1002/rra.1450.

Knack IM, Shen HT, Tuthill AM. 2010. Ice and Sediment Transport in Channels with In-Stream Channel Restoration Structures. In *Proceedings of the 20th IAHR International Symposium on Ice*, Lahti, Finland.

Koskiaho J, Lepistö A, Tattari S, Kirkkala T. 2010. On-line measurements provide more accurate estimates of nutrient loading: a case of the Yläneenjoki river basin, southwest Finland. *Water Science & Technology* **62**: 115–122. DOI: 10.2166/wst.2010.275

Koskinen M. 2008. Erityissuunnitelma Kokemäenjoen tulviin varautumisesta. Lounais-Suomen ympäristökeskus, Suomen ympäristö 12/2008. Edita Prima Oy: Helsinki; 65 pp.

Lawson DE, Chacho EF, Brockett BE, Wuebben JL, Collins CM, Arcone SA, Delaney AJ. 1986. *Morphology, hydraulics and sediment transport of an ice-covered river: field techniques and initial data*. US Army CRREL Report 86–11: Hanover, NH; 37 pp.

Lau Y, Krishnappan B. 1985. Sediment Transport Under Ice Cover. *Journal of Hydraulic Engineering* **111**: 934-950. DOI: doi:10.1061/(ASCE)0733-9429(1985)111:6(934).

Lick W, Jin L, Gailani J. 2004. Initiation of Movement of Quartz Particles. *Journal of Hydraulic Engineering* **130**: 755-761. DOI: 10.1061/(ASCE)0733-9429(2004)130:8(755).

Linjama J, Puustinen M, Koskiaho J. 2009. Implementation of automatic sensors for continuous monitoring of runoff quantity and quality in small catchments. *Agricultural and Food Science* **18**: 417–427.

Lotsari E, Aaltonen J, Veijalainen N, Alho P, Käyhkö J. 2014. Future fluvial erosion and sedimentation potential of cohesive sediments in a coastal river reach of SW Finland. *Hydrological Processes***28**: 6016-6037. DOI: 10.1002/hyp.10080.

Lotsari E, Veijalainen N, Alho P, Käyhkö J. 2010. Impact of climate change on future discharges and flow characteristics of the Tana River, sub-arctic northern Fennoscandia. *Geografiska Annaler: Series A, Physical Geography* **92**: 263–284. DOI: 10.1111/j.1468-0459.2010.00394.x.

Magnuson JJ, Robertson DM, Benson BJ, Wynne RH, Livingstone DM, Arai T, Assel RA, Barry RG, Card V, Kuusisto E, Granin NG, Prowse TD, Stewart KM, Vuglinski VS. 2000. Historical Trends in Lake and River Ice Cover in the Northern Hemisphere. *Science* **289**: 1743–1746. DOI: 10.1126/science.289.5485.1743.

Malve O, Tattari S, Riihimarki J, Jaakkola E, Voss A, Williams R, Baerlund I. 2012. Estimation of diffuse pollution loads in Europe for continental scale modelling of loads and in-stream river water quality. *Hydrological Processes* **26**: 2385–2394. DOI: 10.1002/hyp.9344.

Milburn D, Prowse TD. 1998. Sediment Bound Contaminants in a Remote Northern Delta. *Nordic Hydrology* **29**: 397–414.

Milburn D, Prowse TD. 2002. Under-ice movement of cohesive sediments before river-ice breakup. *Hydrological Processes* **16**: 823-834. DOI: 10.1002/hyp.368.

Moore SA, Ghareh Aghaji Zare S, Rennie CD, Ahmari H, Seidou O. 2013. Monitoring suspended sediment under ice using acoustic instruments: presentation of measurements made during breakup. In *Proceedings of the 17th Workshop on the Hydraulics of Ice Covered Rivers*, Edmonton; 343–354.

Moriasi DN, Arnold JG, Van Liew MW, Bingner RL, Harmel RD, Veith TL. 2007. Model Evaluation Guidelines for Systematic Quantification of Accuracy in Watershed Simulations. *Transactions of the ASABE* **50**: 885-900. DOI: 10.13031/2013.23153.

Muste M, Braileanu F, Ettema R. 2000. Flow and sediment transport measurements in a simulated ice-covered channel. *Water Resources Research* **36**: 2711–2720. DOI: 10.1029/2000WR900168.

Nash JE, Sutcliffe JV. 1970. River flow forecasting through conceptual models part I — A discussion of principles. *Journal of Hydrology* **10**: 282-290. DOI: 10.1016/0022-1694(70)90255-6.

Niinikoski J. 2011. Kokemäenjoen deltan maaperämuodostumat ja niiden vaikutus Porin tulvasuojeluun. Pro Gradu -tutkielma. Turun yliopisto: Turku: 126 pp

Prowse T, Alfredsen K, Beltaos S, Bonsal B, Duguay C, Korhola A, McNamara J, Pienitz R, Vincent W, Vuglinsky V, Weyhenmeyer G. 2011. Past and Future Changes in Arctic Lake and River Ice. *Ambio* **40**: 53–62. DOI: 10.1007/s13280-011-0216-7.

Puustinen M, Tattari S, Koskiaho J, Linjama J. 2007. Influence of seasonal and annual hydrological variations on erosion and phosphorus transport from arable areas in Finland. *Soil and Tillage Research* **93**: 44–55. DOI: 10.1016/j.still.2006.03.011.

Ruosteenoja K, Jylhä K. 2007. Temperature and precipitation projections for Finland based on climate models employed in the IPCC 4th Assessment Report. In *Proceedings of the Third International Conference on Climate and Water*, Heinonen M (ed.),Helsinki; 404–406.

Räike A, Pietiläinen OP, Rekolainen S, Kauppila P, Pitkänen H, Niemi J, Raateland A, Vuorenmaa J. 2003. Trends of phosphorus, nitrogen and chlorophyll a concentrations in Finnish rivers and lakes in 1975–2000. *Science of The Total Environment* **310**: 47–59. DOI: 10.1016/S0048-9697(02)00622-8.

Sayre WW, Song GB. 1979. *Effects of Ice Cover on Alluvial Channel Flow and Sediment Transport Process. Iowa Institute of Hydraulic Research*. The University of Iowa, IIHR Report No. 218, Iowa City, Iowa; 96 pp

Schumm SA. 1973. Geomorphic thresholds and complex response of drainage systems. *Fluvial geomorphology* **6**: 69–85.

Taylor BD. 1971. *Temperature Effects in Alluvial Streams*. California Institute of Tehnology, Report No. KH-R-27: Pasadena, CA; 204 pp.

Turcotte B, Morse B, Bergeron NE, Roy AG. 2011. Sediment transport in ice-affected rivers. *Journal of Hydrology* **409**: 561–577. DOI: 10.1016/j.jhydrol.2011.08.009.

Vehviläinen B. 2007. Hydrological Forecasting and Real-Time Monitoring: The Watershed Simulation and Forecasting System (WSFS). In *Water Quality Measurements Series*, Heinonen P, Ziglio G, Van Der Beken A (eds) John Wiley & Sons Ltd: 13–20.

Vehviläinen B, Huttunen M. 1997. Climate change and water resources in Finland. *Boreal Environment Research* **2**: 3–18.

Veijalainen N, Dubrovin T, Marttunen M, Vehviläinen B. 2010a. Climate Change Impacts on Water Resources and Lake Regulation in the Vuoksi Watershed in Finland. *Water Resources Management* **24**: 3437-3459. DOI: 10.1007/s11269-010-9614-z.

Veijalainen N, Lotsari E, Alho P, Vehviläinen B, Käyhkö J. 2010b. National scale assessment of climate change impacts on flooding in Finland. *Journal of Hydrology* **391**: 333–350. DOI: 10.1016/j.jhydrol.2010.07.035.

Weiss A. 2013. The use of Acoustic Doppler Current Profiler technology to quantify total suspended solids under ice. University of Manitoba, Winnipeg, Manitoba; 201 pp.

Woo M-K, McCann B. 1994. Climatic Variability, Climate Change, Runoff, and Suspended Sediment Regimes in Northern Canada. *Physical Geography* 15; 201–226. DOI: 10.1080/02723646.1994.10642513

Zabilansky LJ, Hains DB, Remus JI. 2006. Increased Bed Erosion Due to Ice. In *Cold Regions Engineering 2006: Current Practices in Cold Regions Engineering*, Davies M, Zufelt JE (eds) American Society of Civil Engineers; 1–12.